AASERT Grant #N00014-93-1-0827

First Semi-Annual Progress Report
(covering the period of 07/15/93-01/15/94)

Project Title: Investigation of a Normal Incidence High-Performance P-type Strained Layer $In_{0.3}Ga_{0.7}As/In_{0.52}Al_{0.48}As$ Quantum Well Infrared Photodetector.

Submitted to

Max N. Yoder

Office of Naval Research
Code 3140
800 North Quincy Street
Arlington, VA 22217-5000

Prepared by

Jerome T. Chu
Student

and

Sheng S. Li
Professor

Department of Electrical Engineering
University of Florida
Gainesville, FL 32611

Tel. (904) 392-4937
Fax (904) 392-8671
E-mail: ShengLi@ENG.UFL.EDU

January 15, 1994

REPORT DOCUMENTATION PAGE

Form Approved
OMB No. 0704-0188

1. AGENCY USE ONLY (Leave blank)	2. REPORT DATE	3. REPORT TYPE AND DATES COVERED
	15 January 1994	Progress Report: 07/15/93-01/15/94

4. TITLE AND SUBTITLE
Investigation of a Normal Incident High Performance P-type Strained Layer $In_{0.3}Ga_{0.7}As/In_{0.52}Ga_{0.48}As$ Quantum Well Infrared Photodetector

5. FUNDING NUMBERS
ONR #N00014-93-1-0827

6. AUTHOR(S)
Jerome T. Chu, Student
Sheng S. Li, Professor

7. PERFORMING ORGANIZATION NAME(S) AND ADDRESS(ES)
University of Florida
Gainesville, FL 32611-6200

8. PERFORMING ORGANIZATION REPORT NUMBER
92120712

9. SPONSORING/MONITORING AGENCY NAME(S) AND ADDRESS(ES)
US Navy, Office of Naval Research
800 North Quincy Street, Code 1512B:SM
Arlington, VA 22217-5000

10. SPONSORING/MONITORING AGENCY REPORT NUMBER

11. SUPPLEMENTARY NOTES

12a. DISTRIBUTION/AVAILABILITY STATEMENT
Approved for public release, distribution unlimited.

12b. DISTRIBUTION CODE

13. ABSTRACT *(Maximum 200 words)*

During this reporting period, we have made significant strides towards the program goals. A major breakthrough was made in the development of a new strained layer p-type InGaAs/InAlAs QWIP grown on InP by MBE. This new QWIP achieved an ultra-low dark current and a very high detectivity at 8.1 um and 77 K. This detector is under background limited performance (BLIP) at temperatures up to 100 K, which is the highest BLIP temperature reported for a QWIP. A dark current density of $7x10^{-8}$ A/cm^2 and a BLIP detectivity of $5.9x10^{10}$ Jones were measured for this QWIP at 77 K. Currently, we are investigating other possible p-type QWIP structures with different performace parameters. These include the design and fabrication of a GaAs/InGaAs p-type QWIP grown on GaAs via MBE and a new dual strained InGaAs/InAlAs p-type QWIP. Additional consideration is being given towards the reliability of p-type contacts for these QWIP structures.

14. SUBJECT TERMS
P-type strained layer InGaAs/InAlAs quantum well infrared photodetectors (QWIPs), intersubband absorption, dark current, responsivity, detectivity.

15. NUMBER OF PAGES

16. PRICE CODE

17. SECURITY CLASSIFICATION OF REPORT	18. SECURITY CLASSIFICATION OF THIS PAGE	19. SECURITY CLASSIFICATION OF ABSTRACT	20. LIMITATION OF ABSTRACT
Unclassified			Unlimited

First Semi-Annual Progress Report (07/15/93-01/15/94)

Project Title: The Development of a Normal Incidence High Performance p-Type Strained Layer $In_{0.3}Ga_{0.7}As/In_{0.52}Al_{0.48}As$ Quantum Well Infrared Photodetectors

Program Manager: Max N. Yoder, Office of Naval Research, Code 3140, Arlington, VA.

Principal Investigator: Sheng S. Li, Professor, University of Florida, Gainesville, FL.

Student : Jerome T. Chu

Project Objective:

The objective of this project is to perform theoretical and experimental studies of dark current, photocurrent, optical absorption, spectral responsivity, noise, and detectivity for the normal incidence strained layer p-type III-V compound semiconductor quantum well infrared photodetectors (QWIPs) developed under this program. The material systems under investigation include InGaAs/InAlAs on InP substrates and GaAs/InGaAs on GaAs substrates. The project will study the usage and effects of biaxial tension and compressional strain on the material systems and their effects towards photodetector design.

I. Introduction

During the period of July 15, 1993 to January 15, 1994, significant progress has been made towards the design, fabrication, and characterization of strained layer p-type InGaAs/InAlAs quantum-well infrared photodetectors (P-QWIPs) in the 8-14 μm range for staring focal plane arrays (FPAs). Specific tasks performed during this period include: (i) the design, growth, fabrication, and characterization of a normal incidence strained-layer p-type InGaAs/InAlAs QWIP on an InP substrate by molecular beam epitaxy (MBE), (ii) the design, growth, and fabrication of a normal incidence strained-layer p-type GaAs/InGaAs QWIP on a GaAs substrate, (iii) the design, growth, and fabrication of a dual strained normal incidence p-type InGaAs/AlGaAs QWIP, and (iv) the design of a two-color dual strained normal incidence p-type InGaAs/AlGaAs QWIP with designed peak responsivity in the 3-5 μm and 8-14 μm bands. The following sections will cover the technical results of the study so far and the research accomplishments and publications.

II. Technical Results

2.1 Research Accomplishments and Publications

1. A new normal incident ultra-low dark current strained layer InGaAs/InAlAs P-QWIP with a $\lambda_p = 8.1$ μm was demonstrated and characterized. The background limited detectivity was found to be 5.9×10^{10} cm-Hz$^{-1/2}$/W at 77 K with BLIP limited operation up to 90 K. These are the highest reported BLIP conditions for a QWIP. The results are summarized later in the text.

2. The design, growth, and fabrication of a compressively strained p-type InGaAs/GaAs QWIP on a GaAs substrate and a dual-strained InGaAs/InAlAs QWIP on an InP substrate to discover the viability of P-QWIPs utilizing the ground state heavy hole to continuum light hole transition and the ground state light hole to continuum light hole transition and the relavent physics.

3. Designed a novel two color dual strained P-QWIP with peak responsivity in the 3-5 μm and 8-14μm ranges. The use of dual strain should allow low dark current and the usage of the heavy hole ground state and first excited state in the quantum well for transitions to the light hole continuum states.

A. Journal Papers:

1. Y. H. Wang, S. S. Li, and J. Chu and Pin Ho, entitled , "An Ultra-low Dark Current P-type Strained-layer InGaAs/InAlAs Quantum Well Infrared Photodetector with Background Limited Performance (BLIP)" accepted *Appl. Phys. Letts*, Feb. 7 issue, 1994.

2. Y. H. Wang, J. Chu and S. S. Li, entitled, "Theoretical and Experimental Studies of a P-type Strained Layer InGaAs/InAlAs QWIP Grown on InP Substrates for 8.1 μm IR Detection", to be submitted to *Journal of Applied Physics*, for publication, Jan. 1994.

B. Conference Presentations:

1. S. S. Li, J. Chu, and Y. H. Wang, "A Normal Incidence P-type Strained Layer InGaAs/InAlAs Quantum Well Infrared Photodetector with Background Limited Performance at 77 K", to be presented at the 1994 SPIE symposium, Orlando, FL, April 5, 1994.

2.2 P-QWIP Operation and Design Theory

N-type quantum well infrared photodetectors have been extensively studied in the recent years[1-2]. These systems use GaAs/AlGaAs and InGaAs/InAlAs structures for detection in the 8 - 14 μm range. Due to the quantum mechanical selection rules which prohibit normal incidence intersubband absorption, focal plane arrays (FPA) using n-type QWIPs must use either metal or dielectric gratings to couple normal incidence IR radiation into the quantum well[2-4]. In contrast, because of mixing between the light hole and heavy hole states, normal incidence illumination is allowed for the intersubband transition in p-type QWIPs.

P-type QWIPs using valence intersubband transitions have been demonstrated[5-7] in lattice-matched GaAs/AlGaAs and InGaAs/InAlAs material systems. In general, intersubband transitions excited by normal incidence radiation in p-type quantum wells are allowed since a linear combination of p-like valence band Bloch states exists, which provides a nonzero coupling between the normal radiation field and valence band Bloch states. The strong mixing between the heavy hole and the light hole states greatly enhances intersubband absorption. The drawback of using lattice-matched systems is the fact that the intersubband transition occurs between the heavy hole ground states and the upper excited states. Because of the relatively large heavy hole effective mass when compared to the electron effective mass, relatively weak absorption and similarly low responsivity are predicted in the IR wavelength range when compared to n-type QWIPs. If biaxial stress is intentionally introduced between the well layers and the barrier layers in the P-QWIP structure, the pseudomorphic or coherent heterointerfaces can be grown if the layer thickness is within the critical thickness. The strained-layers have the same effective in-plane lattice constant, $a_{\|}$ (i.e., $a_{x,y}$), and can store the excess energy due to the elastic strain within the layers. The in-plane lattice constant, $a_{\|}$, can be expressed by[8]

$$a_{\|} = a_1 \left[1 + \delta_o / \left(1 + \frac{\xi_1 L_1}{\xi_2 L_2} \right) \right], \tag{1}$$

where $a_{1,2}$ and $L_{1,2}$ are the individual layer lattice constants and thicknesses, respectively, and $\xi_{1,2}$ are the shear moduli as described by $\xi = (C_{11} + C_{12} - 2C_{12}^2/C_{11})$, where the C_{ij}s are elastic constants for the strained material and can be found in reference 9. δ_o denotes the lattice mismatch between layers, and is defined as $\delta_o = (a_2 - a_1)/a_1$, where a_2 and a_1 are the lattice constants of the strained well and the substrate (or barrier) respectively. If the QWIP structure is grown along the [100] direction and the strained-layer is within the critical thickness, L_c, then the components of the strain tensor [e] are simplified to the expressions given by

$$e_{xx} = e_{yy} = e_{\|} \tag{2}$$

$$e_{zz} = -e_{\|} \left(\frac{2C_{12}}{C_{11}} \right) \tag{3}$$

$$e_{xy} = e_{yz} = e_{zx} = 0. \tag{4}$$

In addition to altering the physical parameters of the QWIP, lattice strain can also induce energy band shifts, which can be used to alter the absorption characteristics of the

QWIP. The strain induced energy band shifts for the conduction band, the heavy hole subband, and light hole subband can be approximated as follows.

$$\Delta E_c = 2c_1 \frac{C_{11} - C_{12}}{C_{11}} \delta_o \tag{5}$$

$$\Delta E_{hh} = b \frac{C_{11} + C_{12}}{C_{11}} \delta_o \tag{6}$$

$$\Delta E_{lh} = -\Delta E_{hh} + \frac{(\Delta E_{hh})^2}{2\Delta_o} \tag{7}$$

where c_1 is the combined hydrostatic deformation potential which characterizes the splitting of the Γ_8 valence band under strain and b is the shear deformation potential and Δ_o is the spin orbit split-off energy[9]. The total hydrostatic deformation potential ($c_1 + V_v$), where V_v is the valence band deformation potential, can be expressed by[10]

$$c_1 + V_v = -\frac{1}{3}(C_{11} + 2C_{12}) \frac{dE_g^o}{dP}, \tag{8}$$

where dE_g^o/dP is the unstrained energy bandgap change with respect to the unit pressure.

The effect of strain on the energy band structure results in the splitting of the heavy hole and light hole band at the valence band zone center[11] (i.e., the in-plane wavevector $k_{||} = 0$), which is degenerate in the unstrained case. When tensile strain is applied between the quantum well and the barrier layers[12-14] along the superlattice growth z-direction, the strain can push the light hole levels upwards and pull the heavy hole levels downwards. We can therefore expect that heavy hole and light hole states can be inverted at specific lattice strains and quantum well thicknesses. This phenomena will in turn cause the intersubband transitions in a QWIP structure to take place from the populated light hole ground state to the upper energy band states. Since the light hole has a small effective mass (comparable to the electron effective mass), the optical absorption and photon responsivity in p-type QWIPs can be greatly enhanced, as a result of introducing strain in the quantum well.

To calculate the locations of the energy subbands, we can use the transfer matrix method (TMM)[13,15], based on the eight-band k·p model. This model is represented by the Luttinger-Kohn Hamiltonian[16-17], H_t, which describes the unstrained semiconductor.

$$H_t = H + V(z) \tag{9}$$

where

$$H = \begin{bmatrix} H_{11} & H_{12} & H_{13} & H_{14} \\ H_{21} & H_{22} & H_{23} & H_{24} \\ H_{31} & H_{32} & H_{33} & H_{34} \\ H_{41} & H_{42} & H_{43} & H_{44} \end{bmatrix} \tag{10}$$

with:

$$H_{11} = \frac{\gamma_1+\gamma_2}{2}(k_x^2 + k_y^2) + \frac{\gamma_1-\gamma_2}{2}k_z^2$$

$$H_{22} = \frac{\gamma_1-\gamma_2}{2}(k_x^2 + K_y^2) + \frac{\gamma_1+\gamma_2}{2}k_z^2$$

$$H_{12} = i\sqrt{3}\gamma_3(k_x - ik_y)k_z$$

$$H_{13} = \frac{\gamma_2\sqrt{3}}{2}(k_x^2 - k_y^2) - i\sqrt{3}\gamma_3 k_x k_y$$

$$H_{21} = H_{12}^*, \qquad H_{13} = H_{31}^*, \qquad H_{24} = H_{13}$$

$$H_{34} = H_{12}, \qquad H_{42}^* = H_{13}, \qquad H_{43} = H_{12}^*$$

$$H_{14} = H_{23} = H_{32} = H_{41} = 0$$

and V(z) is a step function where V(z) vanishes inside the well layers and equals V_o in the barrier layers. The effect of strain is included by adding the Pikus-Bir Hamiltonian[18], H_s, to the general Luttinger-Kohn Hamiltonian. As shown below, the strain Hamiltonian for the well material is a diagonal matrix.

$$H_s = \begin{bmatrix} -\Delta E_c - \Delta E_{hh} & 0 & 0 & 0 \\ 0 & -\Delta E_c + \Delta E_{hh} & 0 & 0 \\ 0 & 0 & -\Delta E_c + \Delta E_{hh} & 0 \\ 0 & 0 & 0 & \Delta E_c + \Delta E_{hh} \end{bmatrix} \tag{11}$$

Using the aforementioned techniques, we can numerically calculate the energy of the zone-center valence subband levels as a function of well width for any material system under tensile or compressional strain and also determine the change in the valence subband structures.

Since the heavy hole and light hole valence subbands are non-degenerate following the introduction of strain into the QWIP structure, a simpler method can be used to determine the energies of the subbands. By using the parabolic band approximation near the valence band zone-center, and the energy band shifts for the conduction band minimum, heavy hole

subband maximum, and light hole subband maximum, we can utilize the simpler two-band Hamiltonian for electrons just by finding the effective mass of the carriers (i.e., heavy hole effective mass and light hole effective mass) and the barrier heights for each carrier type. Although this does not simultaneously determine the energy levels of both carriers, it does allow accurate predictions of the energy subbands. When compared to the direct calculation of the energy subbands, the two-band approximation yields accurate results when compared to the direct calculation results[13,18] (see also figure 1). One limitation of the TMM is that this method cannot calculate the energy levels of the allowed energy subbands in the continuum states. In order to determine the transition energy from the ground state to the continuous state, we used the Kronig-Penney model to determine the locations of the allowed energy bands in the continuum states.

As can be seen in figure 1, the influence of strain on the relative positions of the heavy hole (HH) and light hole (LH) subbands is apparent. When a biaxial internal tension is applied to the well material (in this case $Ga_{0.7}In_{0.3}As$ on an InP substrate with the barrier layers consisting of lattice matched $Al_{0.48}In_{0.52}As$), the strain pulls the LH subbands up with respect to the HH subbands for a given well thickness. While quantum confinement effects tend to push the LH subbands down with respect to the HH subbands. As the well width is increased above a certain value, the strain effect can overcome the quantum confinement effect and therefore induce the inversion of the heavy hole and light hole subbands at the ground state.

In addition to the band structure calculations, one must take into account the optical absorption of the QWIP at the desired wavelength. To find the total linear optical absorption coefficient, we see from the Fermi golden rule that the transition rate from the initial state a to the final state b is expressed as[22]

$$W_{ba} = \frac{2\pi}{\hbar}\left|\left\langle \Psi_b\right| - \frac{q\mathbf{A_0}}{2m_0}\exp(i\mathbf{k}\cdot\mathbf{r})\hat{\epsilon}\cdot\mathbf{p}\left|\Psi_a\right\rangle\right|^2 \times \delta(E_b - E_a - \hbar\omega), \qquad (12)$$

where $\mathbf{A_0}$ is the amplitude of the vector potential, $\mathbf{k}$ is the wave vector of the incoming radiation, $\hat{\epsilon}$ is the polarization vector, m_0 is the free-electron mass, and $\mathbf{p}$ is the momentum vector of the electron in the crystal lattice. Using the effective mass approximation and the assumption that the energy bands are parabolic we see that the envelope function, $\phi(z)$

satisfies the one-dimensional Schrödinger equation:

$$-\frac{\hbar^2}{2m^*}\frac{d^2}{dz^2}\phi(z) + V(z)\phi(z) = E_z(z)\phi(z), \tag{13}$$

where $V(z)$ is the total potential energy of the multi-quantum well structure. The total energy of electrons in the quantum well is given by the sum of the energies parallel and normal to the surface of the quantum well layers, in this case the z-axis, and is given by[24]

$$E_{total} = E_z + \frac{\hbar^2 \mathbf{k}_t^2}{2m^*}, \tag{14}$$

where $\mathbf{k}_t$ is the transverse wave vector in the $x-y$ plane. The electron wave function can be written as[23]

$$\Psi(\mathbf{r}) = \frac{1}{\sqrt{S}}\tilde{u}_c(\mathbf{r})\exp(i\mathbf{k}_t \cdot \mathbf{r}_t)\phi(z), \tag{15}$$

where S is the cross-sectional area of the quantum well, $\mathbf{r}_t$ is the in-plane position vector, and $\tilde{u}_c(\mathbf{r})$ is the cell periodic function of the valence band. To simplify matters, we can assume that there are enough periods of the lattice so that the envelope function can be written in Bloch form as[24]

$$\phi_{nk}(z) = \exp(ikz)u_{nk}(z), \tag{16}$$

where n is the subband index and k is the z component wavevector in the first Brillouin zone, and $k = 2\pi p/NL$ for $-\pi/L \leq k \leq \pi/L$, where N is the number of unit cells in the lattice and p is an integer, and u_{nk} represents the cell periodic function of the lattice, i.e., $u_{nk}(z) = u_{nk}(z + ML)$ where M is an integer.

Using the previous results, we see that the total wave function of the electron in the lattice can be expressed as

$$\begin{aligned} \Psi_a &\equiv \tilde{u}_c(\mathbf{r})F_a(\mathbf{r}), \\ \Psi_b &\equiv \tilde{u}_c(\mathbf{r})F_b(\mathbf{r}) \end{aligned} \tag{17}$$

where

$$\begin{aligned} F_a(\mathbf{r}) &= \frac{1}{\sqrt{S}}\exp(i\mathbf{k}_t \cdot \mathbf{r}_t)\phi_{\alpha k}(z), \\ F_b(\mathbf{r}) &= \frac{1}{\sqrt{S}}\exp(i\mathbf{k}_t \cdot \mathbf{r}_t)\phi_{\beta k}(z). \end{aligned} \tag{18}$$

The subscript a in the previous equation, stands for the quantum numbers (α, $\mathbf{k_t}$, k), and similarly b is defined as (β, $\mathbf{k_t}$,k). For long wavelength intersubband transitions, we can use the dipole approximation ($\mathbf{k} \simeq 0$) so that the matrix element simplifies to

$$\begin{aligned}\left\langle \Psi_b \left| -\frac{q\mathbf{A_0}}{2m_0} \exp(i\mathbf{k}\cdot\mathbf{r}) \right| \Psi_a \right\rangle &\cong \left\langle F_b \left| -\frac{q\mathbf{A_0}}{2m_0} \exp(i\mathbf{k}\cdot\mathbf{r}) \right| F_a \right\rangle \\ &\cong \frac{\mathbf{A_0}}{2i\hbar}(E_a - E_b)\hat{\epsilon}\cdot\langle F_b \left|q\mathbf{r}\right| F_a\rangle \end{aligned} \tag{19}$$

For intersubband transitions, utilizing the assumption that only vertical transitions are allowed, the matrix element of the dipole operator has the following $\mathbf{k_t}$ selection rule[24]

$$\langle F_b \left|q\mathbf{r}\right| F_a\rangle = \delta_{\mathbf{k_p k_t}} q < z > \hat{z}, \tag{20}$$

where

$$< z >= \int_{unit\ cell} u^*_{\beta,k}(z) z u_{\alpha,k} dz. \tag{21}$$

The linear optical absorption coefficient for intersubband transistions can then be stated as follows:[22]

$$\alpha(\hbar\omega) = \frac{1}{V}\sum_{\alpha}\sum_{\beta}\sum_{\mathbf{k_t}}\sum_{\mathbf{k'_t}}\sum_{k} \times \frac{\hbar\omega W_{ba}(f_{\alpha,k} - f_{\beta,k})}{n_r\omega^2 \mathbf{A_0}^2/2\mu c}, \tag{22}$$

where V is the volume of the lattice, n_r is the refractive index, c is the velocity of light, μ is the permeability, and $f_{\alpha,k}$ and $f_{\beta,k}$ are the Fermi-Dirac distribution functions of the upper and lower subbands, respectively. Given the slight inhomogeneities of the well widths and the lifetime broadening due to scattering in the lattice, the Dirac delta function in Eq. (12) can be replaced by a normalized Lorentzian function, $\delta(E) = (\Gamma/2\pi)(E^2 + \Gamma^2/4)^{-1}$; where the linewidth, Γ, can be determined from experimental data. Given these assumptions, the linear absorption coefficient for intersubband transitions can then be expressed as[13,24]

$$\begin{aligned}\alpha(\hbar\omega) &= \sum_{\alpha}\sum_{\beta} \frac{\mu c q^2 \cos^2\theta}{2n_r\hbar\omega N} \sum_{k}[E_\alpha(k) - E_\beta(k)]^2 \\ &\times < z >^2 \frac{m^* k_B T}{L\pi^2} \ln\left(\frac{1 + \exp\{[E_F - E_\alpha(k)]/k_B T\}}{1 + \exp\{[E_F - E_\beta(k)]/k_B T\}}\right) \\ &\times \frac{1}{\pi}\frac{\Gamma/2}{[E_\beta(k) - E_\alpha(k) - \hbar\omega]^2 + (\Gamma/2)^2}, \end{aligned} \tag{23}$$

where θ is the angle between the polarization direction and the z axis.

Although our band structure and absorption calculations can be used to determine the positions of the subbands in the quantum wells, and hence determine the peak absorption wavelength of the QWIP, many other factors must be taken into account to create a successful detector. Generally, for a useful detector, the responsivity must be high, while the noise current must be low. The responsivity, R, for a photodetector may be expressed as[19]

$$R = \frac{q\lambda\eta p}{hc} G, \tag{24}$$

where q is the electronic charge, λ is the wavelength of the incident photon, h is the Planck constant, c is the speed of light, p is the tunneling probability out of the quantum well, η is the quantum efficiency and the photoconductive gain is G. The quantum efficiency and photoconductive gain are described, respectively, by[19]

$$\eta = A\left[1 - exp\left(-B\alpha l_{qw}\right)\right] \tag{25}$$

$$G = \frac{L}{t_c} \tag{26}$$

where A is a constant that is polarization dependent, α is the absorption coefficient of the quantum well, l_{qw} is the total width of all quantum well regions, L is the mean free path of the carrier, and t_c is the total width of all quantum well and barrier regions. B is a constant dependent on the number of passes IR radiation makes through the photodetector. For n-type QWIPs, A=0.5, while for p-type QWIPs A=1. The mean free path of the carrier may be expressed as[19]

$$L = \tau T_{qw} \mu_{eff} E, \tag{27}$$

where τ is the well recapture lifetime of the carrier, T_{qw} is the transmission coefficient over the quantum well, μ_{eff} is the effective mobility of the carrier, and E is the electric field. The effective mobility for a two-band transport model is shown to be[19]

$$\mu_{eff} = \frac{\Delta p_{lh}\mu_{lh} + \Delta p_{hh}\mu_{hh}}{\Delta p_{lh} + \Delta p_{hh}}, \tag{28}$$

where Δp_{hh} and Δp_{lh} are the concentrations of optically induced heavy and light hole carriers respectively, and μ_{hh} and μ_{lh} are the respective heavy and light hole mobilities. When only the ground state is completely occupied, either Δp_{lh} or Δp_{hh}, the optically induced light holes or the optically induced heavy holes dominate, so that we may estimate μ_{eff} as the in-plane effective mass of the ground state carriers.

Another important parameter to be considered in a QWIP design is the dark current density (J_d), which is expressed using the Richardson-Dushman equation[14] as

$$J_d \propto T^2 m^* exp\left(\frac{-\Delta E}{kT}\right), \tag{29}$$

where m^* is the effective mass, ΔE is the difference in energy between the barrier height and the quantum confined state in the well, k is the Boltzmann constant, and T is the temperature.

The noise in QWIP structures is mainly due to random fluctuations of thermally excited carriers. The noise is expressed as[5]

$$i_{noise} = \sqrt{4A_d qG\Delta f J_d}, \tag{30}$$

where A_d is the detector area, and Δf id the bandwidth. Finally, a figure of merit measurement used to compare detectors is the detectivity, D^*, which is shown to be[19]

$$D^* = \sqrt{A_d \Delta f}\frac{R}{i_{noise}}. \tag{31}$$

If the dark current in a particular QWIP is lower than the 300 K background photocurrent, then the QWIP can be considered to be under background limited performance (BLIP). In a BLIP limited QWIP, the dominant current is due to photon noise, since all the other sources are negligible by comparison. The photon noise is calculated from the arrival statistics of the incoherent photons. The background photon noise current, i_{np}, is given by[20,21]

$$i_{np}^2 = 4Aq^2\eta g^2 P_b B/(h\nu), \tag{32}$$

where P_b is the incident background optical power, B is the QWIP bandwidth, η is the absorption quantum efficiency, ν is the incident photon frequency, and g is the photoconductive gain. The photocurrent, I_p can be approximated by

$$I_p = A(q/h\nu)\eta g P_s, \tag{33}$$

where P_s is the incident optical signal power. The constant, A, in Eqs. (32) and (33), is due to the polarization selectivity for n-type QWIPs versus p-type QWIPs. As previously stated, for n-type QWIPs, A = 0.5, while A = 1 for p-type QWIPs. By setting the signal-to-noise

power ratio equal to unity, the background limited noise equivalent power, $(NEP)_{BLIP}$ and the detectivity, D^*_{BLIP}, can be expressed as follows for n-type QWIPs.

$$(NEP)_{BLIP} = 2\sqrt{2h\nu BP_b/\eta} \tag{34}$$

$$D^*_{BLIP} = \sqrt{A_d B}/(NEP)_{BLIP} = \frac{\lambda_p}{2\sqrt{2}hc}\left(\frac{\eta}{Q_b}\right)^{1/2}, \tag{35}$$

where A_d is the active area of the detector, and $Q_b = P_b/(Ah\nu)$ is the incident photon flux from the background for a given spectral bandwidth, $\Delta\nu$, and a peak wavelength, λ_p. Q_b is defined as

$$Q_b = \frac{2\pi}{c^2}\frac{\nu^2\Delta\nu}{e^{h\nu/k_bT}-1}sin^2\left(\frac{\theta}{2}\right), \tag{36}$$

where, θ, is the field of view (FOV). For a p-type QWIP, a factor of $\sqrt{2}$ is used in the denominator of Eq. (35), D^*_{BLIP}, since it can absorb both optical polarizations of the incident IR radiation.

2.3 Characterization of Strained Layer P-QWIPs

As can be seen in figure 1, we can utilize the strain inherent in a lattice mismatched system in addition to the engineering of the well thicknesses and barrier layers to modify the energy band structure of the p-type QWIPs. The strained-layer $In_{0.3}Ga_{0.7}As/In_{0.52}Al_{0.48}As$ P-QWIP as shown in figure 2, uses a light hole ground state to heavy hole continuum state intersubband transition for IR detection. The QWIP structure was grown on a (100) semi-insulating InP substrate via molecular beam expitaxy (MBE). Beryllium was used as the p-type dopant and the structure consists of 20 periods of 4 nm thick $In_{0.3}Ga_{0.7}As$ quantum wells with a dopant density of $1x10^{18}$ cm^{-3} seperated by 45 nm thick barrier layers of undoped $In_{0.52}Al_{0.48}As$ barrier layers. A 0.3 μm thick cap layer and a 1 μm thick buffer layer of $In_{0.53}Ga_{0.47}As$ were grown with a dopant density of $2x10^{18}$ cm^{-3} to serve as ohmic contacts. The contact and barrier layers were designed to be lattice matched with the InP substrate. The quantum wells are in biaxial tension with a lattice mismatch of 1.6% between the well layers and the substrate. A 200 μm by 200 μm mesa was then created by chemical etching to facilitate the measurement of spectral responsivity and dark current of the QWIP. A Au/Zn alloy was used to make ohmic contacts to the p-type QWIP. The ohmic contacts

were thermally evaporated onto the QWIP mesas to a thickness of 0.12 μm. The QWIPs were annealed at 480 ° C for two minutes to obtain stable and low contact resistance.

Figure 3 shows the measured dark current density from 77 K to 110 K with a 300 K background photocurrent superimposed. The asymmetric dark current characteristic in this p-type QWIP was observed due to the band bending in the barrier layers as shown in Fig. 2. Due to the extremely low dark current density of this QWIP, it is under background limited performance (BLIP) for a field of view (FOV) of 90° at a temperature less than 90 K under applied biases from -2.5 V to +5 V and higher. In the forward biased regime, the QWIP is under BLIP operation up to 100 K with an applied bias of +2.5 V.

The responsivity of the QWIP can be measured as a function of temperature, applied bias, and incident radiation wavelength. Using a globar and an automatic PC-controlled single grating monochrometer, under normal incidence infrared (IR) radiation, we can measure the photocurrent versus radiation wavelength for both positive and negative biases; which are shown in figures 4 and 5, respectively. A peak wavelength at λ_p=8.1 μm was observed in the long wavelength infrared detection band, which is attributed to the intersubband transition between the confined ground light hole state and the continuum heavy hole states. The cutoff wavelength was found to be 8.8 μm which corresponds to a spectral bandwidth of $\Delta\lambda/\lambda_p$ = 12%. The responsivities for the p-type QWIP were calibrated using a standard pyroelectric detector and lock-in amplifier. Asymmetric responsivities of 34 mA/W and 51 mA/W at +4 V and -4 V bias, respectively, were measured. The maximum BLIP detectivity, D^*_{BLIP}, at λ_p=8.1 μm was determined to be 5.9x10^{10} cm-Hz$^{1/2}$/W with a responsivity, R of 18 mA/W at +2 V bias with a FOV = 90° at 77 K. The quantum efficiency for the p-type QWIP was estimated from the responsivity measurements using a conservative photoconductive gain estimate of g=0.015. The %BLIP can be evaluated as follows when the Johnson noise and readout noise are ignored; with i_{np} and i_{nd} are the 300 K background photocurrent noise and dark current noise, respectively.

$$\%BLIP \approx \frac{i_{np}}{(i_{np}^2 + i_{nd}^2)^{1/2}} \tag{37}$$

Using the above expression, a nearly full BLIP detection was achieved at biases with magnitudes less than 2 V, as seen in figure 6. Due to the BLIP detection, the noise equivalent temperature difference (NEΔT) is expected to be improved significantly for this QWIP.

The two new single color QWIP structures are designed to explore the utilization of the intersubband transistions from the heavy hole ground state to the light hole continuum states for the compressively strained p-type InGaAs/GaAs on GaAs substrate QWIPs, and from the light hole ground state to the light hole continuum states for the dual strained p-type InGaAs/InAlAs on InP substrate QWIPs. The compressively strained P-QWIP is designed to utilize the high density of states in the heavy hole ground state to enhance absorption while conduction in the QWIP itself uses the light hole continuum states, which should enhance the time response of the QWIP. The dually strained P-QWIP design is meant to explore the enhancement that is predicted for the linear absorption coefficient, due to the light hole ground state. This device also uses the light hole continuum states which should also enhance the time response of the QWIP.

Finally, a new two-color dually strained P-QWIP has been designed to utilize intersubband transitions to provide two band detection in the 3-5 and 8-12 μm ranges without the need to switch detection modes. This design also utilizes the high density of states in the heavy hole ground state to improve absorption while hole conduction is due to the light hole continuum states, so as to provide a faster time response.

2.4 Conclusion and Remarks

Over the last half-year period, we have achieved a greater understanding in regards to the design and characterization of P-QWIPs. We have demonstrated a novel strained-layer design with ultra-low dark current, high detectivity, high responsivity, and BLIP operation. Current research involves the continuation of the aforementioned strained layer P-QWIP study along with the exploration of optimized designs for enhanced device performance, along with the study of a two-color design utilizing intersubband transitions in the 3-5 and 8-14 μm ranges.

References

1. B. F. Levine, R. J. Malik, J. Walker, K. K. Choi, C. G. Bethea, D. A. Kleinman, and J. M. Vandenberg, Appl. Phys. Lett. **50**, 273 (1987).

2. L. S. Yu, S. S. Li, Appl. Phys. Lett. **59**, 1332 (1991).

3. G. Hasnain, B. F. Levine, C. G. Bethea, R. A. Logan, J. Walker, and R. J. Malik, Appl. Phys. Lett. **54**, 2515 (1989).

4. J. Y. Andersson and L. Lundqvist, J. Appl. Phys. **71**, 3600 (1992).

5. B. F. Levine, S. D. Gunapala. J. M. Kuo, S. S. Pei, and S. Hui, Appl. Phys. Lett. **59**, 1864 (1991).

6. J. Katz, Y. Zhang, and W. I . Wang, Electron. Lett. **28**, 932 (1992).

7. W. S. Hobson, A. Zussman, B. F. Levine, and J. deJong, J. Appl. Phys. **71**, 3642 (1992).

8. J. W. Matthews and A. E. Blakeslee, J. Cryst. Growth **32**, 265 (1976).

9. Landolt-B(o)rnstein, Numerical Data and Functional Relationships in Science and Technology, O. Madelung, ed., Group III, **17a, 22a**, Springer-Verlag, Berlin (1986).

10. G. Ji, D. Huang, U. K. Reddy, T. S. Henderson, R. Houre, and H. Morkoç, J. Appl. Phys. **62**, 3966 (1987).

11. T. P. Pearsall, Semiconductors and Semimetals, **32**, 55 (1990).

12. H. Asai, and Y. Kawamura, Appl. Phys. Lett. **56**, 746 (1990).

13. H. Xie, J. Katz, and W. I. Wang, Appl. Phys. Lett. **59**, 3601 (1991).

14. R. T. Kuroda and E. Garmire, Infrared Phys. **34**, 153 (1993).

15. L. R. Ram-Mohan, K. H. Yoo, and R. L. Aggarwal, Phys. Rev B **38**, 6151 (1988).

16. J. M. Luttinger and W. Kohn, Phys. Rev. **97**, 869 (1956).

17. J. M. Luttinger, Phys. Rev. **102**, 1030 (1956).

18. G. L. Bir and G. E. Pikus, Symmetry and Strain-Induced effects in Semiconductors, Wiley, New York (1974).

19. E. L. Derniak and D. G. Crowe, Optical Radiation Detectors, Wiley, New York (1984).

20. B. F. Levine, C. G. Bethea, G. Hasnain, J. Walker, and R. J. Malik, Appl. Phys. Lett. **53**, 296 (1988).

21. D. A. Scribner, M. R. Kruer, and J. M. Killiany, Proc. of the IEEE **79**, 66, (1991).

22. D. Ahn and S. L. Chuang, Phys. Rev. B **24**, 4149 (1987).

23. M. Altarelli, in *Heterojunctions and Semiconductor Superlattices*, edited by G. Allen, G. Bastard, N. Boccara, M. Lannoo, and M. Voos, Springer, New York (1986).

24. K. T. Kim, S. S. Lee, and S. L. Chuang, J. Appl. Phys. **69**, 6617 (1991).

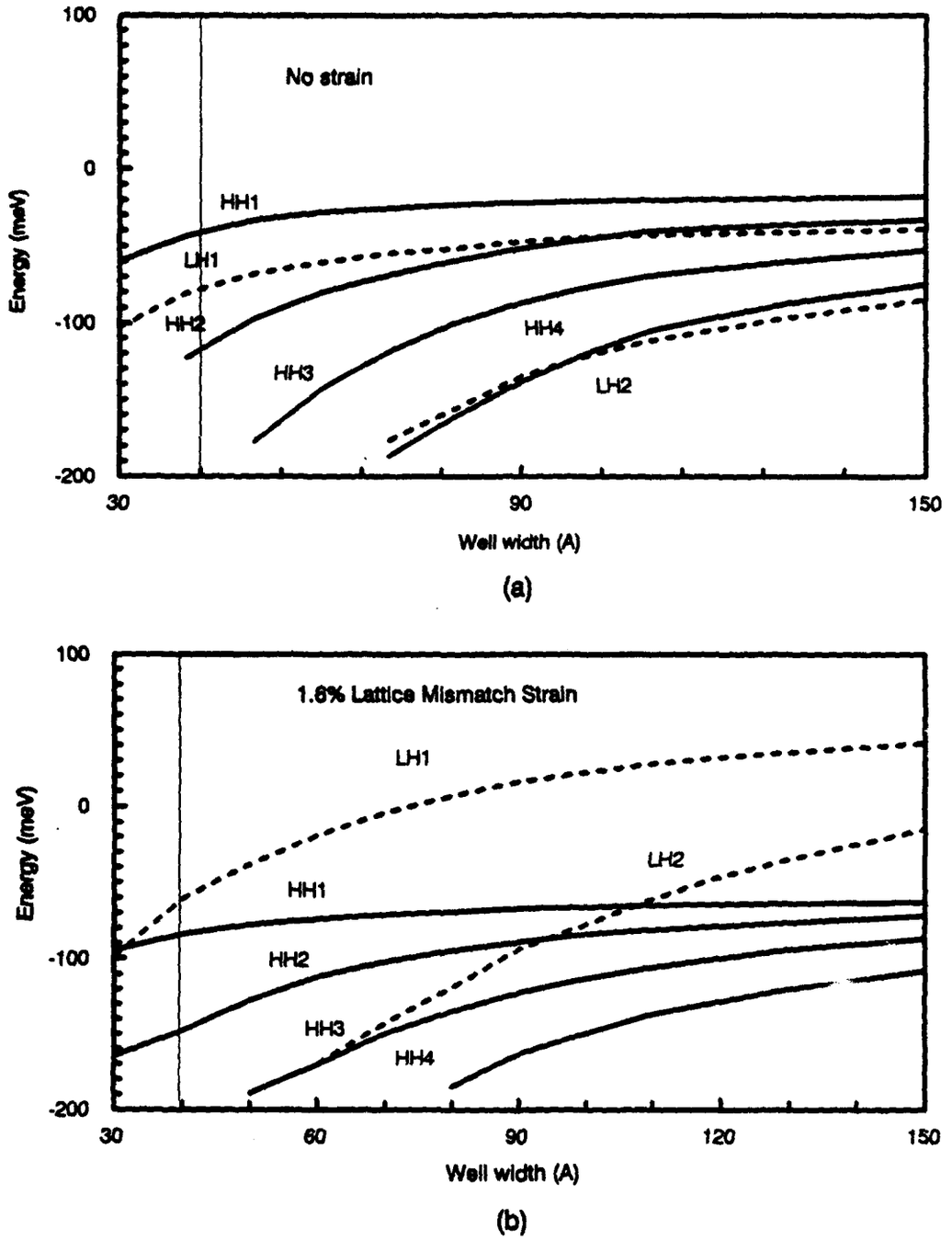

Figure 1: Energy band structure at the valence band zone-center for an $In_{0.3}Ga_{0.7}As/In_{0.52}Al_{0.48}As$ SL P-QWIP as a function of well thickness (a) without and (b) with the effects of strain (valence band offset of 140 meV).

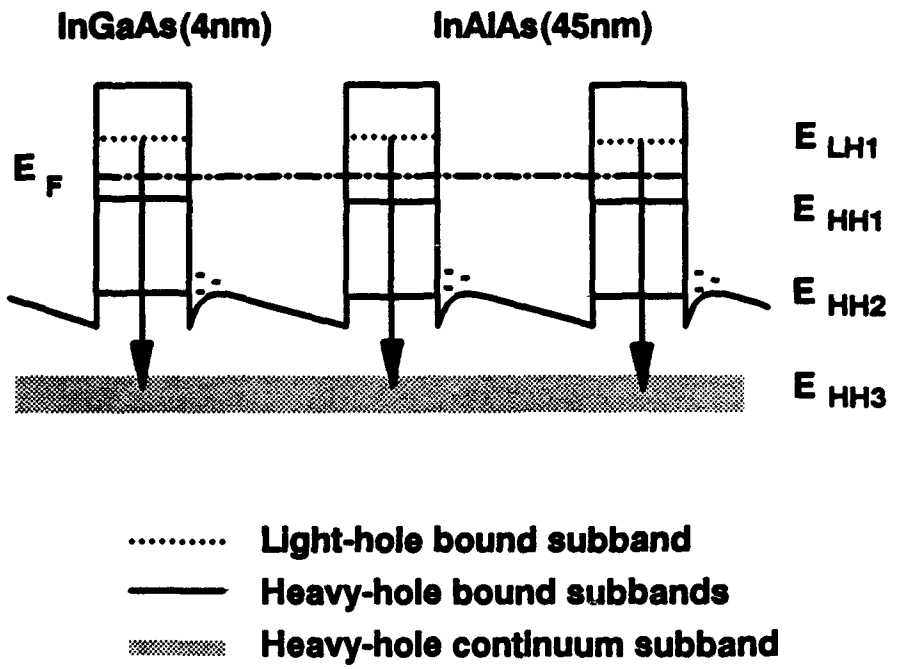

Figure 2: Schematic energy band structure for the strained layer $In_{0.3}Ga_{0.7}As/In_{0.52}Al_{0.48}As$ P-QWIP.

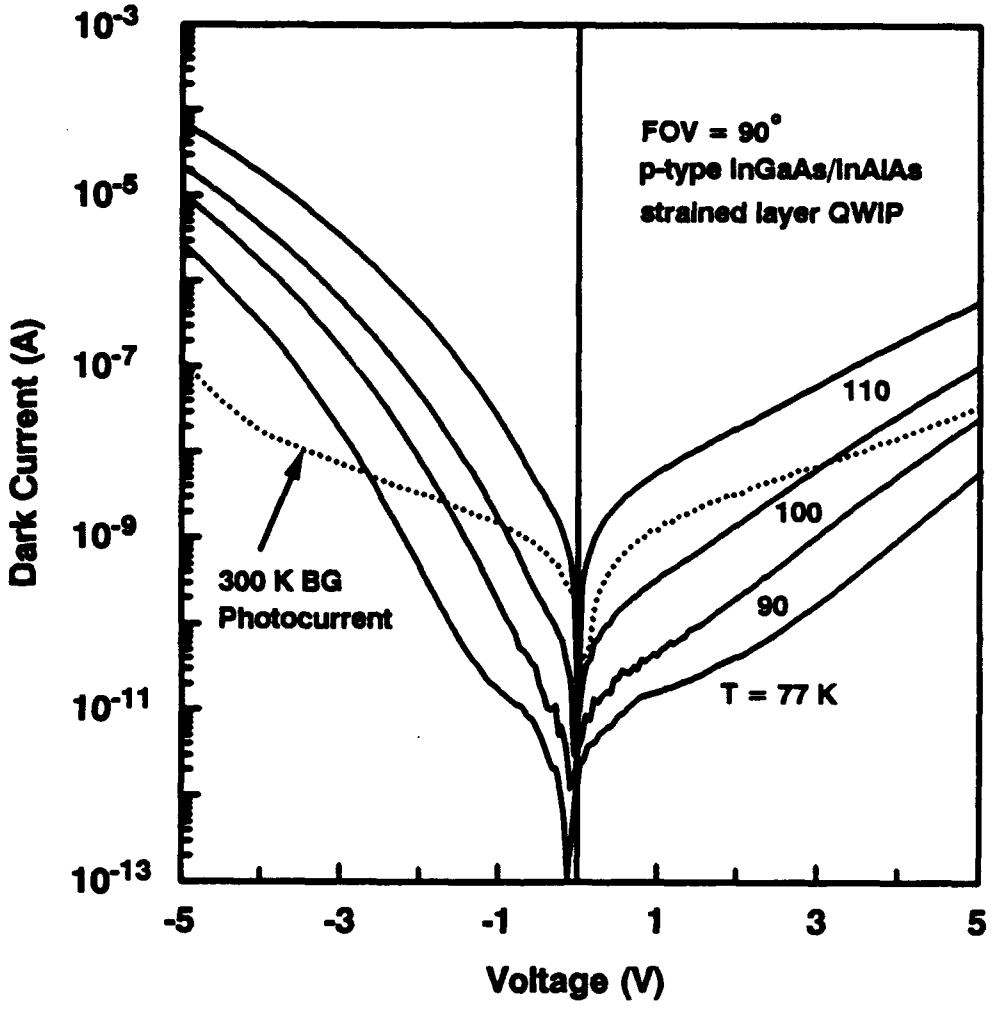

Figure 3: Dark current characteristics of the InGaAs/InAlAs P-QWIP as a function of temperature and applied bias compared with the 300 K background photocurrent.

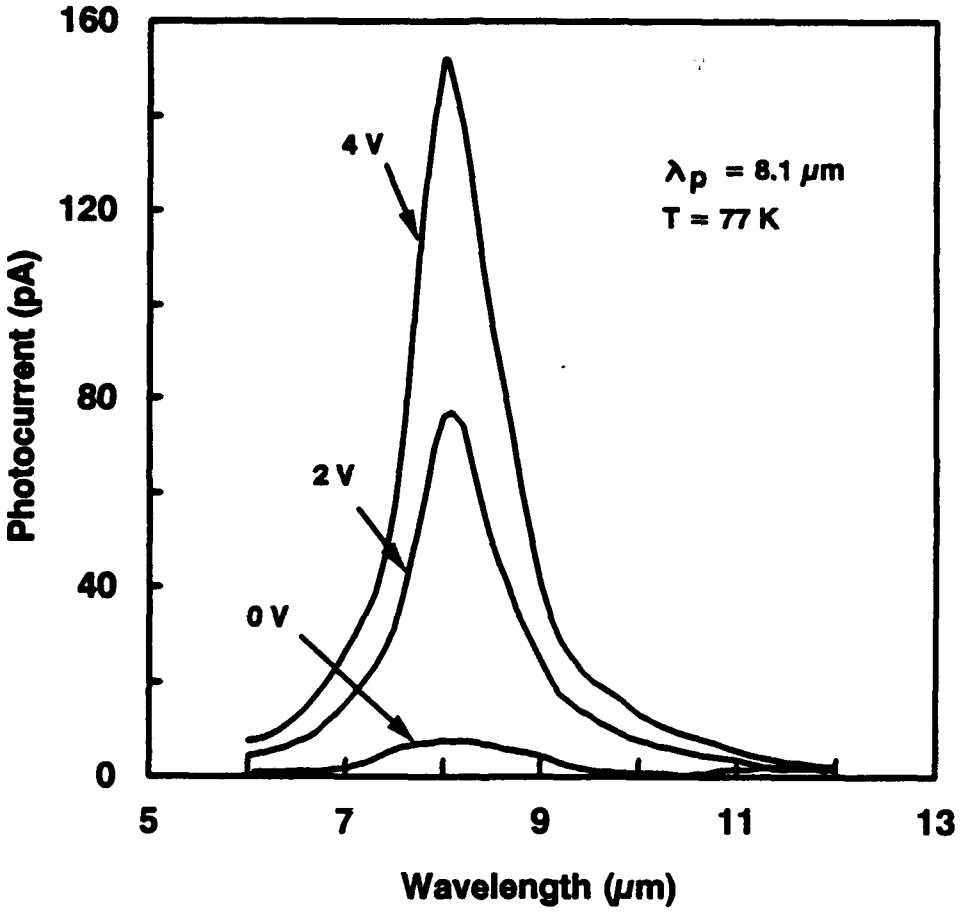

Figure 4: Measured photocurrent versus wavelength for different positive applied biases for the p-type $In_{0.3}Ga_{0.7}As/in_{0.48}Al_{0.52}As$ QWIP.

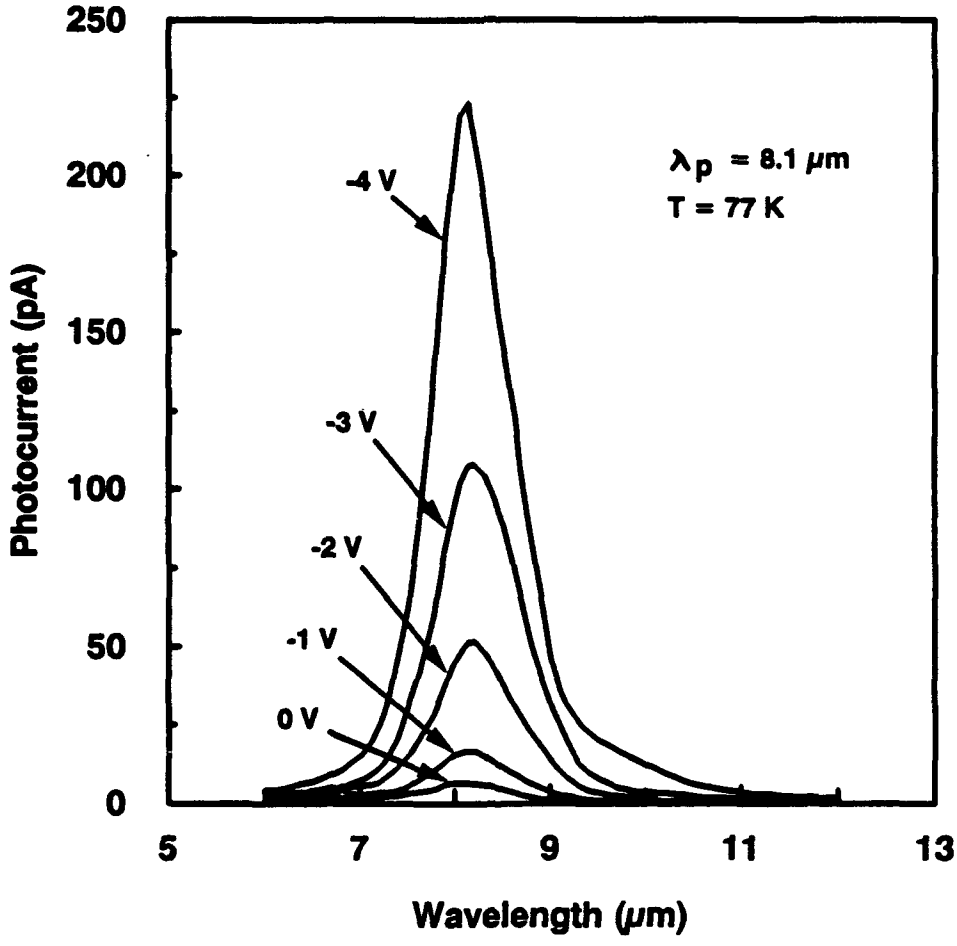

Figure 5: Measured photocurrent versus wavelength for different negative applied biases for the p-type $In_{0.3}Ga_{0.7}As/In_{0.48}Al_{0.52}As$ QWIP.

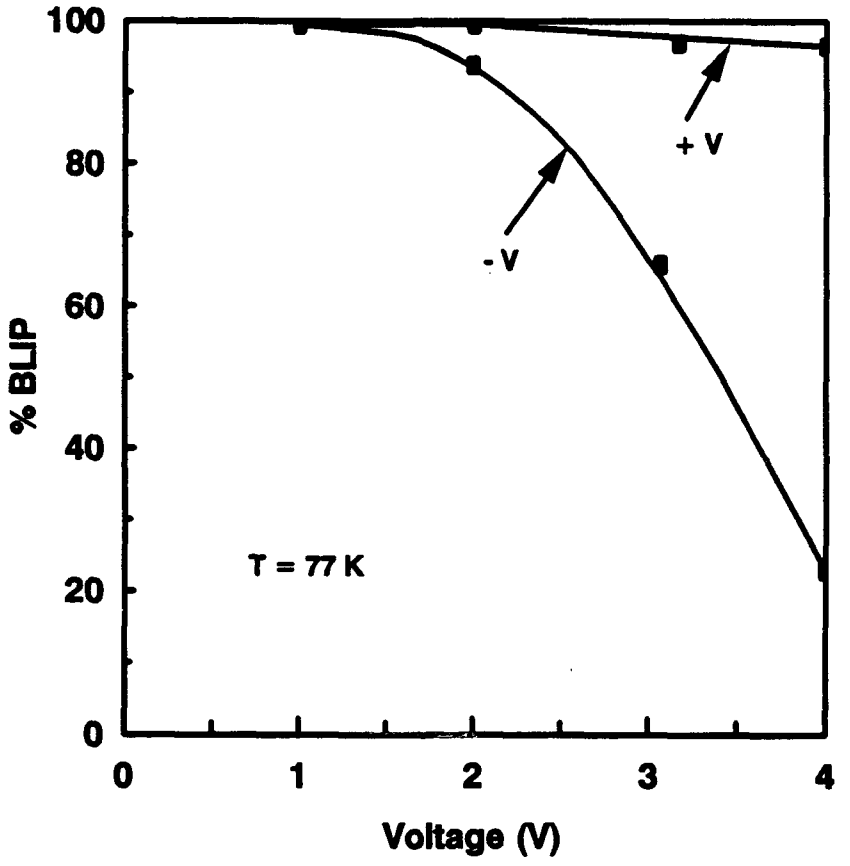

Figure 6: The %BLIP as a function of applied bias for the InGaAs/InAlAs P-QWIP at 77 K.

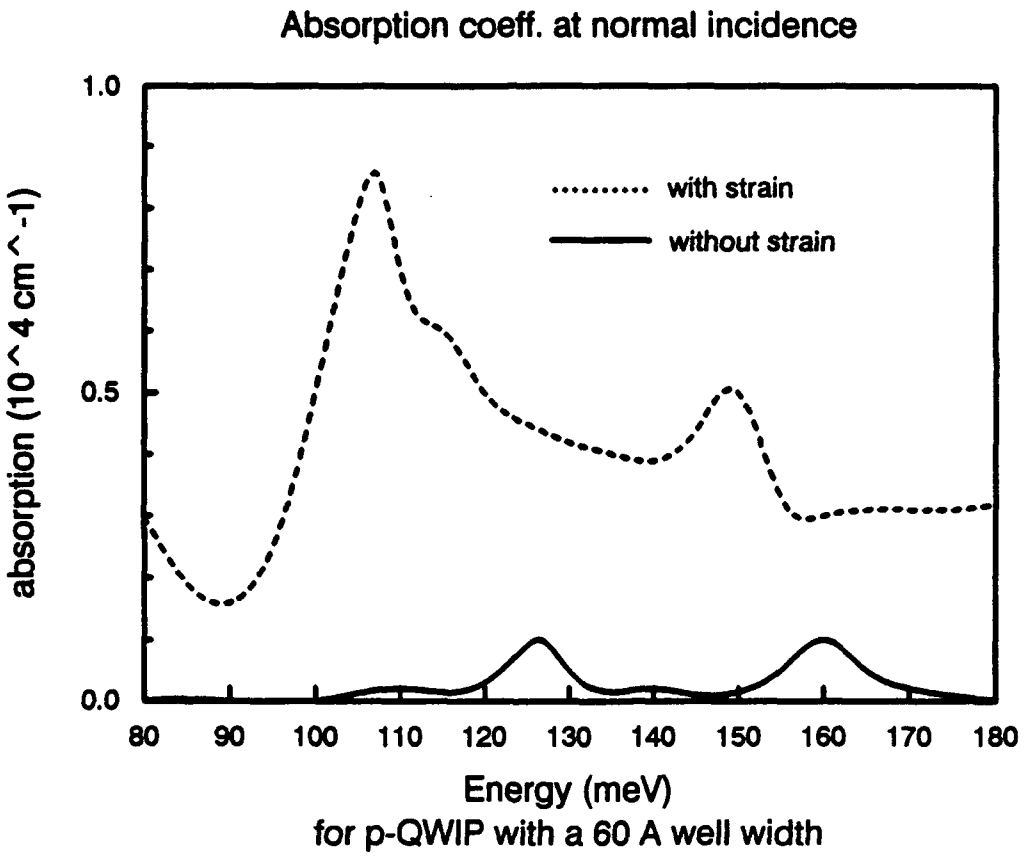

Figure 7: The calculated absorption coefficient at normal incidence as a function of photon energy for the InGaAs/InAlAs P-QWIP.